RESEARCH ARTICLE SUMMARY

NEURODEVELOPMENT

A latent lineage potential in resident neural stem cells enables spinal cord repair

Enric Llorens-Bobadilla, James M. Chell, Pierre Le Merre, Yicheng Wu, Margherita Zamboni, Joseph Bergenstråhle, Moa Stenudd, Elena Sopova, Joakim Lundeberg, Oleg Shupliakov, Marie Carlén, Jonas Frisén*

INTRODUCTION: The capacity of a tissue to regenerate itself rests on the potential of its resident cells to replace cells lost to injury. Some tissues, such as skin or intestine, do this remarkably well through the activation of tissue-specific stem cells. Injuries to the central nervous system (CNS), in contrast, often lead to permanent functional impairment; some cells lost to injury are never replaced. Neural stem cells have been identified in the adult brain and spinal cord and are activated by injury. However, injury-activated neural stem cells predominantly produce scar-forming astrocytes, and the contribution of neural stem cells to cell replacement is insufficient for regeneration. To design regenerative strategies aimed at recruiting resident neural stem cells for repair, it is essential to know whether greater regenerative potential exists and how to elicit such potential.

RATIONALE: The spinal cord is a great system to study neural stem cell recruitment for repair. The neural stem cell potential of the spinal cord resides in a well-characterized population of ependymal cells. Ependymal cells, normally quiescent, are activated by injury to generate almost exclusively scar-forming astrocytes. Ependymal-derived astrocytes help to preserve tissue integrity, but other cell types, such as myelin-forming oligodendrocytes, are insufficiently replaced. In parallel, neural stem cell transplantation has proven to be beneficial to recovery after spinal cord injury—a benefit that is associated with the increased supply of oligodendrocytes able to remyelinate demyelinated axons. Ependymal cells share a developmental origin with spinal oligodendrocytes, which led us to explore whether a latent potential for expanded oligodendrocyte generation might exist.

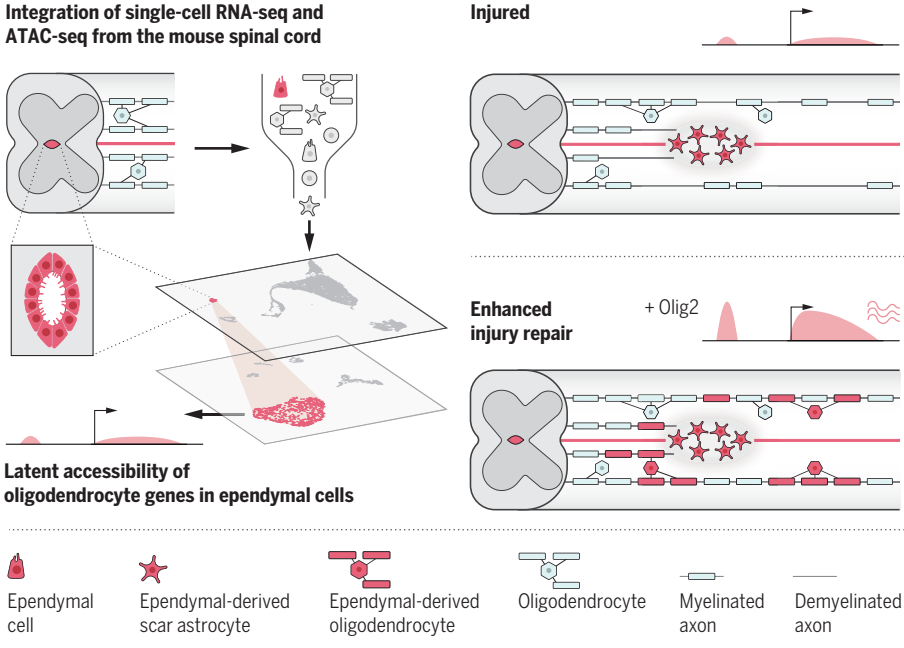

Latent potential in neural stem cells. Through the integration of different layers of genomic information in single cells, we found that the genetic program for oligodendrocyte generation is latently accessible in ependymal neural stem cells of the adult spinal cord. After injury, activating the latent potential by forced OLIG2 expression unfolds efficient oligodendrocyte generation, leading to enhanced repair.

RESULTS: We integrated single-cell RNA sequencing (scRNA-seq) and single-cell assay for transposase-accessible chromatin using sequencing (scATAC-seq) to study lineage potential in adult ependymal cells of the mouse spinal cord. We found that the genetic program for oligodendrocyte generation is accessible in ependymal cells. However, this program is latent, as oligodendrocyte genes are not expressed. In particular, we found that a large fraction of binding sites for OLIG2, the transcription factor that initiates developmental oligodendrogenesis, had basal accessibility, despite OLIG2 and its key target genes not being expressed in adult ependymal cells. To study whether this latent accessibility was associated with a greater capacity to produce oligodendrocytes, we genetically engineered a mouse model to express OLIG2 in adult ependymal cells. We found that OLIG2 expression was compatible with ependymal identity during homeostasis. However, after injury, OLIG2 expression led to the increased accessibility of the latent program and subsequent expression of genes specifying oligodendrocyte identity. Unfolding of the latent program was followed by efficient oligodendrocyte production from ependymal cells, but not from astrocytes, after injury. Using scRNA-seq of ependymal-derived cells, we found that new oligodendrocytes followed the developmental program of oligodendrocyte maturation, including a self-amplifying oligodendrocyte progenitor cell–like state. These cells later matured to acquire the identity of resident mature myelinating oligodendrocytes. Further, ependymal oligodendrocyte generation occurred in parallel and not at the expense of astrocyte scarring. Newly recruited ependymal-derived oligodendrocytes migrated to sites of demyelination, where they remyelinated axons over the long term. Finally, using optogenetics, we found that ependymal-derived oligodendrocytes contributed to normalizing axon conduction after injury.

CONCLUSION: Adult neural stem cells have a greater potential for regeneration than is normally manifested. Targeted activation of such potential leads to the recruitment of neural stem cells for the generation of remyelinating oligodendrocytes in numbers comparable to those obtained via cell transplantation. Resident stem cells can thus serve as a reservoir for cellular replacement and may offer an alternative to cell transplantation after CNS injury. ■

The list of author affiliations is available in the full article online.
*Corresponding author. Email: jonas.frisen@ki.se
Cite this article as E. Llorens-Bobadilla *et al.*, *Science* **370**, eabb8795 (2020). DOI: 10.1126/science.abb8795

RESEARCH ARTICLE

NEURODEVELOPMENT

A latent lineage potential in resident neural stem cells enables spinal cord repair

Enric Llorens-Bobadilla[1], James M. Chell[1]*, Pierre Le Merre[2], Yicheng Wu[1], Margherita Zamboni[1], Joseph Bergenstråhle[3], Moa Stenudd[1], Elena Sopova[2], Joakim Lundeberg[3], Oleg Shupliakov[2,4], Marie Carlén[2,5], Jonas Frisén[1]†

Injuries to the central nervous system (CNS) are inefficiently repaired. Resident neural stem cells manifest a limited contribution to cell replacement. We have uncovered a latent potential in neural stem cells to replace large numbers of lost oligodendrocytes in the injured mouse spinal cord. Integrating multimodal single-cell analysis, we found that neural stem cells are in a permissive chromatin state that enables the unfolding of a normally latent gene expression program for oligodendrogenesis after injury. Ectopic expression of the transcription factor OLIG2 unveiled abundant stem cell–derived oligodendrogenesis, which followed the natural progression of oligodendrocyte differentiation, contributed to axon remyelination, and stimulated functional recovery of axon conduction. Recruitment of resident stem cells may thus serve as an alternative to cell transplantation after CNS injury.

The adult mammalian central nervous system (CNS) has a limited capacity for regeneration after injury, and functional impairments typically persist permanently (*1*). Resident neural stem cells exist in the brain and spinal cord, but they show a propensity to generate an astrocyte scar at the expense of multilineage cell replacement after injury, leading to regeneration failure (*2*–*5*). Recruiting endogenous stem cells for cell replacement has become one of the main goals of regenerative medicine in the CNS (*6*), but whether greater regenerative potential exists remains unknown.

Latent accessibility of the regulatory program for oligodendrogenesis in spinal cord ependymal cells

The stem cell potential of the spinal cord resides in the small population of ependymal cells (*7*–*9*). To explore the lineage potential of ependymal cells, we performed single-cell assay for transposase-accessible chromatin using sequencing (scATAC-seq) (*10*) of resident non-neuronal cell populations in the mouse spinal cord, enriching for ependymal cells during sorting (Fig. 1A and supplementary materials). We directly compared our scATAC-seq profiles of 1100 cells with single-cell RNA sequencing (scRNA-seq) of the same tissue (fig. S1) (*11*). Integration of the promoter and gene body accessibility in scATAC-seq together with marker gene expression in scRNA-seq led to the identification of clusters of ependymal cells, astrocytes, oligodendrocyte progenitor cells, vascular endothelial cells, and pericytes in our scATAC-seq dataset (Fig. 1, B and C, and fig. S2, A to F), thus capturing the major scar-forming cell populations in the spinal cord (*2*). Besides the concordance that promoter and gene body accessibility showed with RNA expression, differential accessibility analyses identified 17,000 regulatory regions with cluster-specific accessibility patterns (fig. S2, G and H). Motif enrichment analyses on cluster-specific regulatory regions revealed high enrichment of predicted transcription factors, such as regulatory factor X (RFX) factors for ependymal cells (*12*) (Fig. 1D). We observed that the motifs for the canonical oligodendrocyte lineage transcription factors OLIG2 and SOX10 were highly accessible not only in oligodendrocyte progenitor cells (OPCs) but also in ependymal cell clusters (Fig. 1D). This was unexpected, as OLIG2 and SOX10 are expressed in oligodendrocyte lineage cells but not in adult ependymal cells (Fig. 1E and fig. S3) (*8*). To further explore this observation, we examined the accessibility of oligodendrocyte-lineage transcription factor loci, including SOX10, a factor essential for oligodendrogenesis with some previously characterized regulatory regions (*13*, *14*). We noted that a conserved SOX10 enhancer (28 kb upstream) accessible in OPCs also showed accessibility in ependymal cells, but less in other clusters (Fig. 1E). A similar pattern was observed in multiple other oligodendrocyte lineage genes (fig. S4, A to D). The SOX10 enhancer contained an OLIG2 binding site (Fig. 1F), which led us to explore whether accessibility at OLIG2 binding sites was a more general phenomenon. Indeed, OLIG2 binding sites accessible in oligodendrocyte progenitors were also highly enriched in the accessible landscape of ependymal cell clusters, despite OLIG2 not being expressed (Fig. 1G). The genetic program for oligodendrogenesis is thus permissive in ependymal cells despite the lack of expression of its critical regulators.

Expression of OLIG2 in ependymal cells leads to activation of the latent oligodendrocyte lineage program after injury

OLIG2 initiates developmental oligodendrogenesis upstream of SOX10, with the expression of SOX10 marking the irreversible commitment to the oligodendrocyte lineage (*15*, *16*). To study whether introducing the expression of OLIG2 in adult ependymal cells would lead to the deployment of the permissive oligodendrocyte program, we generated Rosa-CAG-LSL-Olig2-IRES-tdTomato (Olig2-tdT) mice for conditional and simultaneous expression of OLIG2 and tdTomato upon cre-mediated recombination (fig. S5A). To express OLIG2 specifically in ependymal cells and their progeny, we crossed Olig2-tdT mice to Foxj1-creER mice, generating Foxj1-Olig2-tdT mice, with Foxj1-tdT serving as control mice (Fig. 2A). Tamoxifen induction led to OLIG2 expression in all recombined cells at levels ~5 times those in nonrecombined OLIG2-expressing parenchymal cells (Fig. 2B and fig. S5B). We first performed ATAC-seq on isolated ependymal cells from uninjured Foxj1-tdT and Foxj1-Olig2-tdT mice. In addition, to study the ependymal response to injury at the chromatin level, we also isolated cells 1 or 5 days after a dorsal funiculus incision injury (Fig. 2C), when the ependymal cell progeny begin to mobilize toward the injury site but still express ependymal markers (fig. S5, C to E). To define the associated transcriptional programs, we performed RNA-seq on matched samples collected in parallel (fig. S6). Comparative analysis revealed high concordance between the global chromatin accessibility of ependymal cells from uninjured Foxj1-tdT and Foxj1-Olig2-tdT mice, with increasingly different profiles after injury (Fig. 2D). To study changes in the activity of the oligodendrocyte gene expression program, we measured the accessibility of OPC-enriched regions that contained OLIG2 binding sites in ependymal cells (1560 regions; Fig. 2E). Although the accessibility did not increase in ependymal cells from uninjured mice in the presence of OLIG2, these sites rapidly gained accessibility after injury in OLIG2-expressing ependymal cells [increases by factors of 1.5 and 1.9 at 1 and 5 days post-injury (dpi), respectively; Fig. 2F]. Increased accessibility was also observed in the complete set of OPC-enriched regions, and the OLIG2 motif was highly enriched in all the regions

[1]Department of Cell and Molecular Biology, Karolinska Institutet, SE-171 77 Stockholm, Sweden. [2]Department of Neuroscience, Karolinska Institutet, SE-171 77 Stockholm, Sweden. [3]Science for Life Laboratory, Karolinska Institutet Science Park, SE-171 21 Solna, Sweden. [4]Institute of Translational Biomedicine, St. Petersburg State University, 199034 St. Petersburg, Russia. [5]Department of Biosciences and Nutrition, Karolinska Institutet, SE-141 83 Huddinge, Sweden.
*Present address: 10X Genomics, Södra Fiskartorpsvägen 15C, SE-114 33 Stockholm, Sweden.
†Corresponding author. Email: jonas.frisen@ki.se

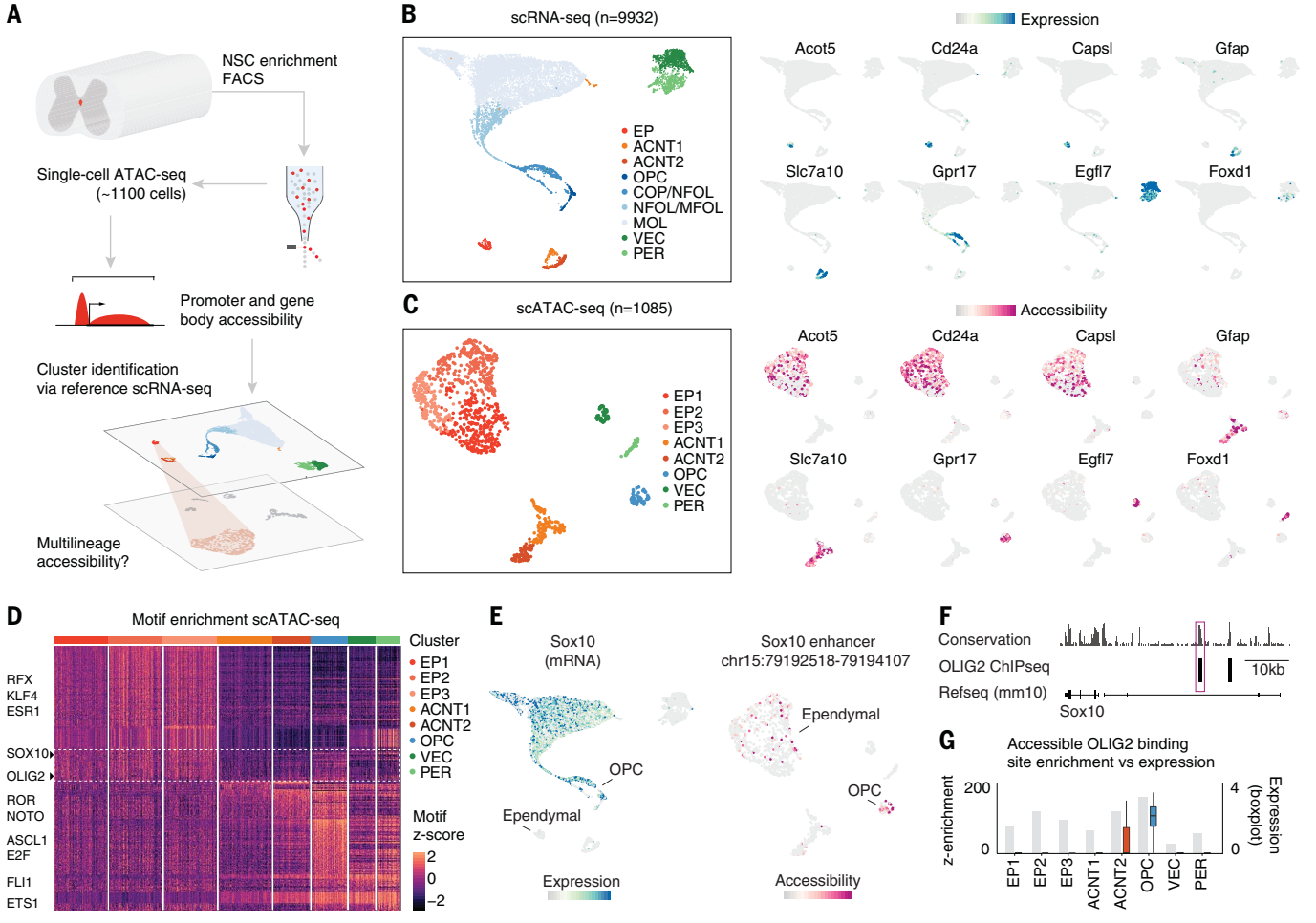

Fig. 1. Integration of scRNA-seq and scATAC-seq uncovers latent accessibility of the oligodendrocyte lineage program in ependymal cells. (**A**) scATAC-seq was performed on non-neuronal cells from the mouse spinal cord. Ependymal neural stem cells (NSCs) were enriched during fluorescence-activated cell sorting (FACS; see supplementary materials). Genes with variable promoter and gene body accessibility were identified and used as anchors to reference cell types identified in scRNA-seq. (**B**) UMAP projection of non-neuronal spinal cord single-cell transcriptomes from (*11*). Clusters were annotated according to the reference atlas (*11*). EP, ependymal; ACNT, non-telencephalon astrocyte; OPC, oligodendrocyte progenitor cell; COP, committed oligodendrocyte progenitor; NFOL, newly formed oligodendrocyte; MFOL, myelin-forming oligodendrocyte; MOL, mature oligodendrocyte; VEC, vascular endothelial cell; PER, pericyte. The expression of cluster-specific markers is projected on UMAP on the right. (**C**) UMAP projection of non-neuronal spinal cord cell transcriptomes assayed by scATAC-seq. Clusters were annotated according to the correspondence between gene accessibility and scRNA-seq expression (fig. S1). The accessibility of representative cluster-specific markers is projected on UMAP on the right. (**D**) Heat map showing motif enrichment in genomic regions with cluster-specific accessibility. Scaled enrichment scores for the top 100 motifs per cluster are shown. OLIG2 and SOX10 motifs show enrichment in OPCs and ependymal clusters (arrowheads at left). (**E**) Expression of SOX10 is restricted to cells from the oligodendrocyte lineage, whereas a 28-kb upstream enhancer of SOX10 is accessible in OPCs and in ependymal cells. (**F**) The enhancer, highlighted in magenta, is highly conserved (shown in the placental mammal phastCons track) and contains an OLIG2 binding site. ChIP, chromatin immunoprecipitation. (**G**) Enrichment for OLIG2 binding sites in the accessible-chromatin landscape of ependymal cells. Gray bars show Z enrichments; box plots show OLIG2 expression in the respective clusters.

that gained accessibility after injury (fig. S5, F to I), which suggests that accessibility gains in the oligodendrocyte program were a direct consequence of OLIG2 binding. Accessibility gains were greater in oligodendrocyte lineage regions than in regions defining astrocyte or vascular cell clusters, suggesting specificity (fig. S5H), and led to nascent expression of the nearest genes (fig. S5J). Further, regions that gained accessibility included several upstream enhancers of SOX10, and accessibility in those regions was highly correlated with the onset of SOX10 expression (Fig. 2, G and H) and the subsequent accessibility of its target sites (fig. S5K). Together, these findings show that the program for oligodendrogenesis has a latent accessibility in ependymal cells and that this latent program can be rapidly unveiled in the presence of OLIG2 in response to injury.

Activation of the latent oligodendrocyte program leads to efficient oligodendrocyte production after injury

Oligodendrocytes are vulnerable to CNS damage, and oligodendrocyte loss leads to the dysmyelination of spared and regenerated axons after spinal cord injury (*17*, *18*). We next asked whether the increased accessibility of the oligodendrocyte lineage program in ependymal cells would lead to the generation of oligodendrocytes during injury repair (Fig. 3A). As previously described, injury induced a vigorous ependymal cell response characterized by proliferation and migration of the ependymal cell progeny to the lesion site in Foxj1-tdT mice (Fig. 3, B and C). The tdTomato-labeled progeny in Foxj1-tdT mice consisted almost exclusively of cells expressing the astrocyte marker SOX9, which contributed to the formation of the glial

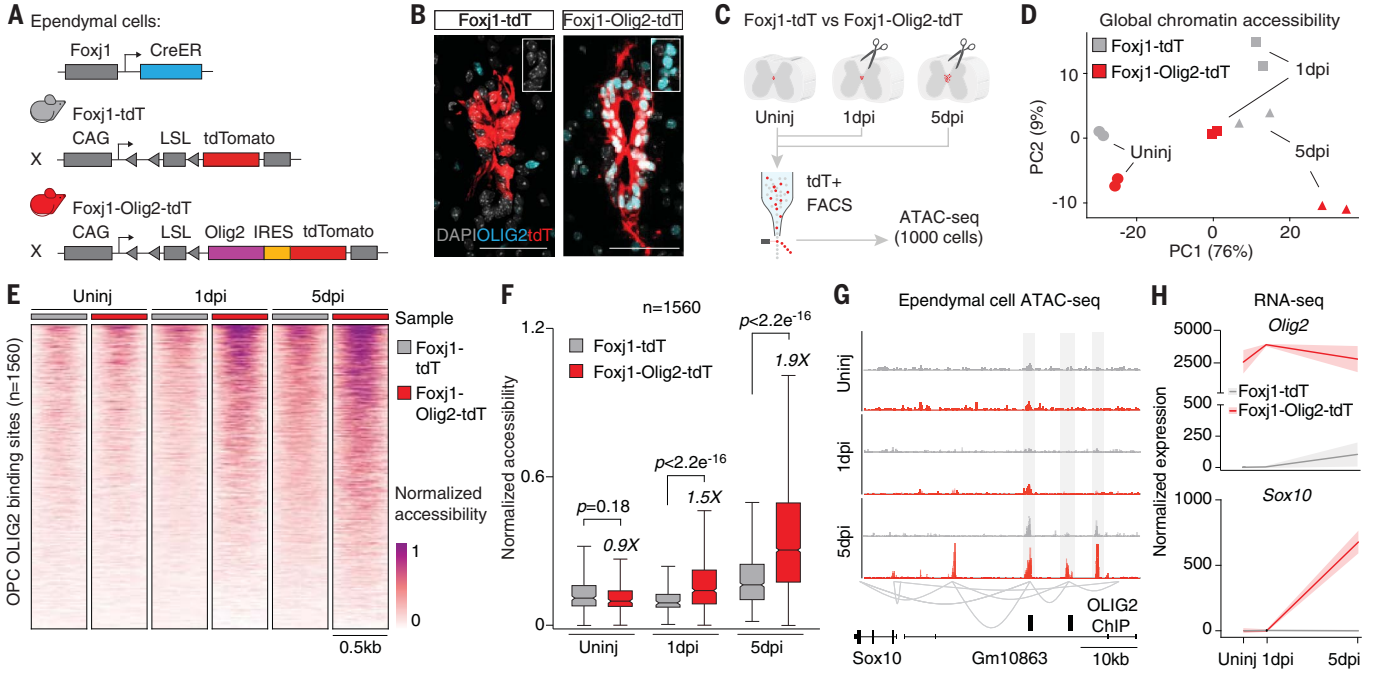

Fig. 2. The latent oligodendrogenic program in ependymal cells unfolds after injury in the presence of OLIG2. (**A**) Schematic representation of the experimental design for fate mapping of ependymal cells and induction of OLIG2 expression in recombined cells. (**B**) OLIG2 immunostaining shows the absence of expression in Foxj1-tdT ependymal cells and uniform nuclear expression in Foxj1-Olig2-tdT cells. Insets show magnification of ependymal cells. Scale bar, 50 μm. (**C**) We isolated tdTomato$^+$ (tdT) cells from tamoxifen-injected Foxj1-tdT and Foxj1-Olig2-tdT mice at different time points after a dorsal funiculus incision injury (uninjured, 1 dpi, and 5 dpi) and performed ATAC-seq. (**D**) Principal components analysis of the global chromatin accessibility profiles of cells from Foxj1-tdT and Foxj1-Olig2-tdT mice. (**E**) Normalized genomic accessibility (ATAC-seq counts per million) heat map for OPC-enriched genomic regions containing OLIG2 binding sites. Regions were scaled to 0.5 kb; each lane represents the average of two replicates. (**F**) Tukey box plots showing the accessibility of regions in (E) reveal a rapid increase in accessibility in OLIG2-expressing ependymal cells after injury. *P* values are from Kruskal-Wallis test followed by Dunn's post hoc test. (**G**) Genomic tracks showing normalized accessibility (scale 0 to 1.5) upstream of SOX10. Sample colors as in (F). (**H**) Expression of OLIG2 and SOX10 by RNA-seq (n = 2; lines and shaded regions denote means ± SD).

scar (Fig. 3C and fig. S7A). Consistent with previous observations (*8*), we also detected a low number of cells expressing the oligodendrocyte lineage (OL) marker SOX10 (<1% of the ependymal cell progeny) 4 weeks after injury (fig. S7C).

In line with the lack of chromatin accessibility changes prior to injury, recombined ependymal cells in Foxj1-Olig2-tdT mice remained by the central canal and retained their normal morphology in the absence of injury (Fig. 3D). However, after injury, OLIG2-expressing ependymal cells generated a large number of SOX10-positive cells, in addition to generating astrocytes in the scar (Fig. 1E). Four weeks after injury, these SOX10-positive oligodendroglial cells were abundant, constituting ~30% of the ependymal cell progeny (fig. S7, B and C). We refer to these cells as ependymal-derived oligodendrocyte lineage cells (epOLs) to distinguish them from other parenchymal oligodendrocyte lineage cells. We followed the process of epOL generation over time; this revealed a progressive generation of SOX10$^+$ tdT$^+$ cells (11,000 ± 3000 cells 12 weeks after injury) (Fig. 3F and fig. S7, D and E), which corresponds to an increase in oligodendroglial cell production from ependymal cells by a factor of >40. In parallel, relative to Foxj1-tdT mice at 2, 4, and 12 weeks after injury, the total numbers of ependymal cell progeny in Foxj1-Olig2-tdT mice increased by factors of 1.3, 2.2, and 2.7, respectively (Fig. 3G); this finding suggests that epOL generation did not occur at the expense of astrocyte generation and did not lead to ependymal cell depletion (fig. S7, F to H). Interestingly, forced OLIG2 expression in parenchymal astrocytes failed to elicit efficient oligodendrogenesis after injury (fig. S8), supporting the view that ependymal cells are specifically permissive to oligodendrogenesis.

Ependymal-derived oligodendrogenesis molecularly recapitulates developmental oligodendrogenesis and is compatible with astrocyte generation

We next sought to molecularly reconstruct ependymal oligodendrogenesis at single-cell resolution. For this, we isolated tdTomato$^+$ cells from three cohorts of Foxj1-tdT and Foxj1-Olig2-tdT mice: uninjured, 2 weeks after injury, and 4 weeks after injury (Fig. 3A). Cells were then profiled using droplet-based 3′ single-cell RNA sequencing (scRNA-seq). After sequencing and filtering (fig. S9, A to D), we recovered a total of ~3000 single-cell transcriptomes. Computational analyses revealed the presence of six clusters organized in two main groups, one defined by *Sox9* expression (four clusters) and the other one by *Sox10* expression (two clusters; Fig. 3, H to J). The first cluster of *Sox9*-expressing cells contained the vast majority of cells from uninjured Foxj1-tdT and Foxj1-Olig2-tdT mice and expressed the highest levels of ependymal markers (e.g., *Rarres2*, *Cd27*, *Nnat*). We denote this cluster as ependymal (EP). Ependymal cells from uninjured Foxj1-tdT and Foxj1-Olig2-tdT mice clustered tightly together, which suggests that OLIG2 had only a mild influence on the ependymal cell transcriptome in the absence of injury (Fig. 3K).

The other three clusters of *Sox9*-expressing cells were enriched in the ependymal cell progeny from both Foxj1-tdT and Foxj1-Olig2-tdT mice 2 and 4 weeks after injury, which progressively shifted in the t-distributed stochastic neighbor embedding (tSNE) space (Fig. 3, H and K, and fig. S9F). Cells in these clusters were characterized by up-regulation of astrocyte markers (e.g., *Vim*, *Gfap*, *Cryab*) and concomitant down-regulation of ependymal markers (Fig. 3,

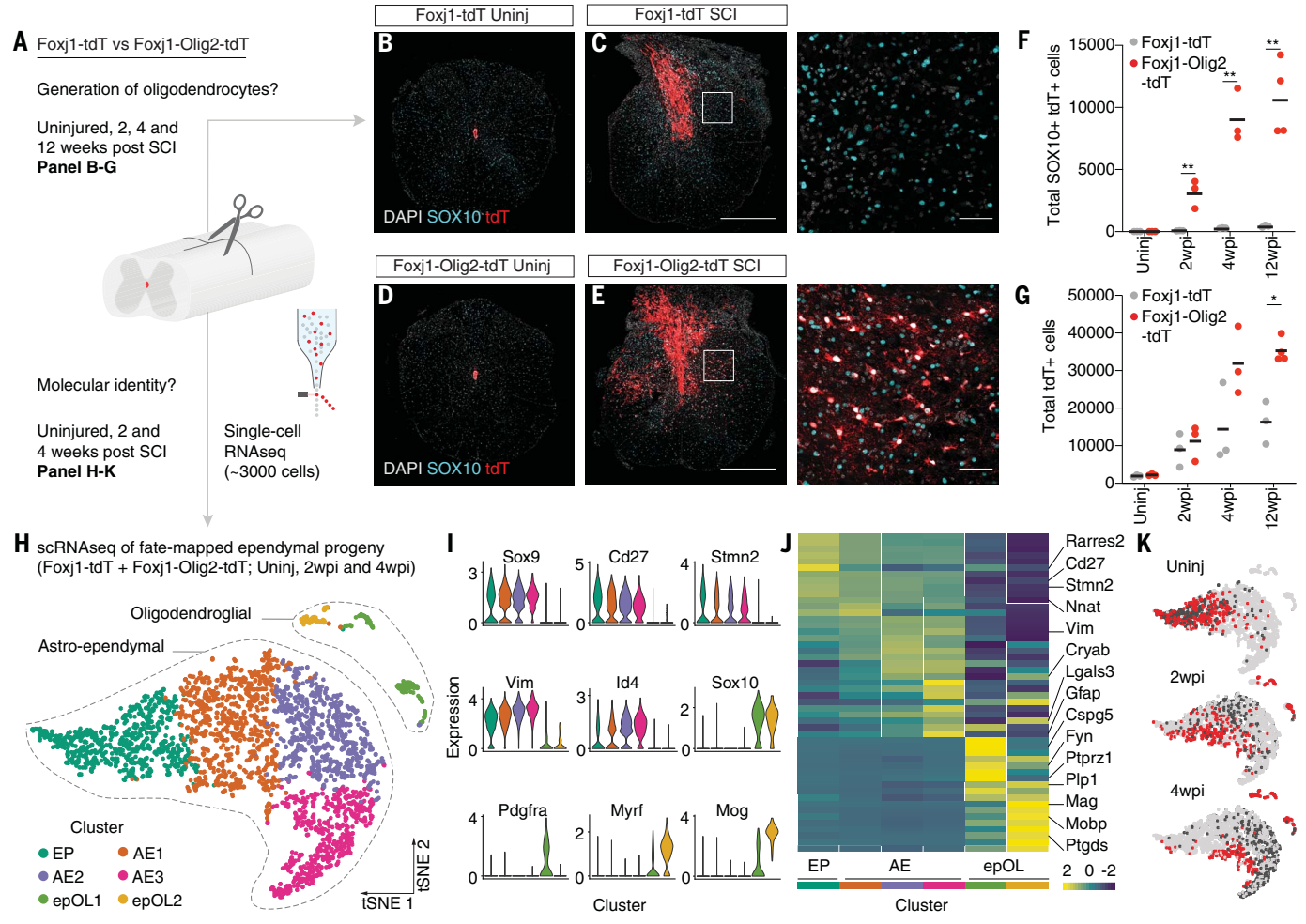

Fig. 3. Ependymal cells can generate abundant oligodendrocytes after injury. (**A**) Schematic representation of the experimental design to assess ependymal oligodendrogenesis. SCI, spinal cord injury. (**B** to **G**) The spinal cord was analyzed 2, 4, and 12 weeks after injury. (B) Coronal view of an uninjured spinal cord at the thoracic level in a Foxj1-tdT mouse, showing specific recombination in ependymal cells. (C) Coronal view of the Foxj1-tdT spinal cord 4 weeks after injury, showing scar formation from ependymal cell progeny. At right, magnification of the box in (C). (D) Coronal view of an uninjured spinal cord at the thoracic level in a Foxj1-Olig2-tdT mouse, showing specific recombination in the ependymal layer and absence of migration. (E) Coronal view of the Foxj1-Olig2-tdT spinal cord 4 weeks after injury, showing abundant SOX10$^+$ tdT$^+$ cells. At right, magnification of the box in (E). (F) Quantification of ependymal-derived oligodendrocytes in Foxj1-tdT and Foxj1-Olig2-tdT mice uninjured and 2, 4, and 12 weeks post-injury (wpi) (n = 3 or 4). Total numbers of cells in the injured segment are shown (see supplementary materials). (G) Quantification of the total numbers of ependymal-derived cells in Foxj1-tdT and Foxj1-Olig2-tdT mice uninjured and 2, 4, and 12 wpi in the injured segment (n = 3 or 4). Horizontal bar in (F) and (G) denotes the mean. *P < 0.05, **P < 0.01 [one-way analysis of variance (ANOVA) followed by Tukey post hoc test]. (**H** to **K**) The identity of the ependymal progeny was assessed by scRNA-seq 2 and 4 weeks after spinal cord injury. (H) tSNE visualization of the single-cell transcriptomes of all tdT$^+$ cells (Foxj1-tdT and Foxj1-Olig2-tdT; uninjured, 2 and 4 wpi) color-coded by cluster: EP, ependymal; AE, astroependymal; epOL, ependymal-derived oligodendrocyte lineage. (I) Violin plots showing the expression of representative cluster-specific genes. *Sox9* and *Sox10* demarcate the two main cell groups (EP-AE and epOL). OL clusters are defined by the expression of immature (*Pdgfra*) and mature (*Myrf*, *Mog*) oligodendrocyte lineage markers. (J) Heat map of the average scaled expression of the top cluster-specific genes. For the full list of top marker genes, see data S1. (K) tSNE visualization of the identity of fate-mapped ependymal cells split by sampling time and colored by genotype.

I and J). Gene Ontology analysis indicated that cells in these clusters up-regulated programs for cell division, migration, gliogenesis, and response to wounding, in line with being scar-forming cells (fig. S10, A and B). We named these clusters astroependymal 1 to 3 (AE1, AE2, and AE3) to reflect the ependymal origin and acquisition of astroglial identity.

Expression of *Sox10* defined the other two clusters (Fig. 3I), which corresponded to the epOLs identified above. These cells did not express the ependymal or astroependymal programs, and the acquisition of oligodendroglial identity was fully supported by Gene Ontology analyses (fig. S10, C and D). The epOL cells were absent in uninjured mice and emerged after injury almost exclusively in Foxj1-Olig2-tdT mice (38% of Foxj1-Olig2-tdT and 0.4% of Foxj1-tdT cells 4 weeks after injury) (Fig. 3K and fig. S9E).

When visualized using diffusion maps, cells from Foxj1-Olig2-tdT mice (uninjured, 2 weeks after injury, and 4 weeks after injury, respectively) were organized along two divergent paths, with cells from the ependymal cluster enriched at the vertex, and AE3 and epOL2 cells enriched at the respective branch ends (Fig. 4, A and B). Pseudotime score determined with the diffusion map closely reflected time after injury (Fig. 4, C and D) and further supported AE3 and epOL2 as the terminal differentiation states of the divergent branches of ependymal cell differentiation.

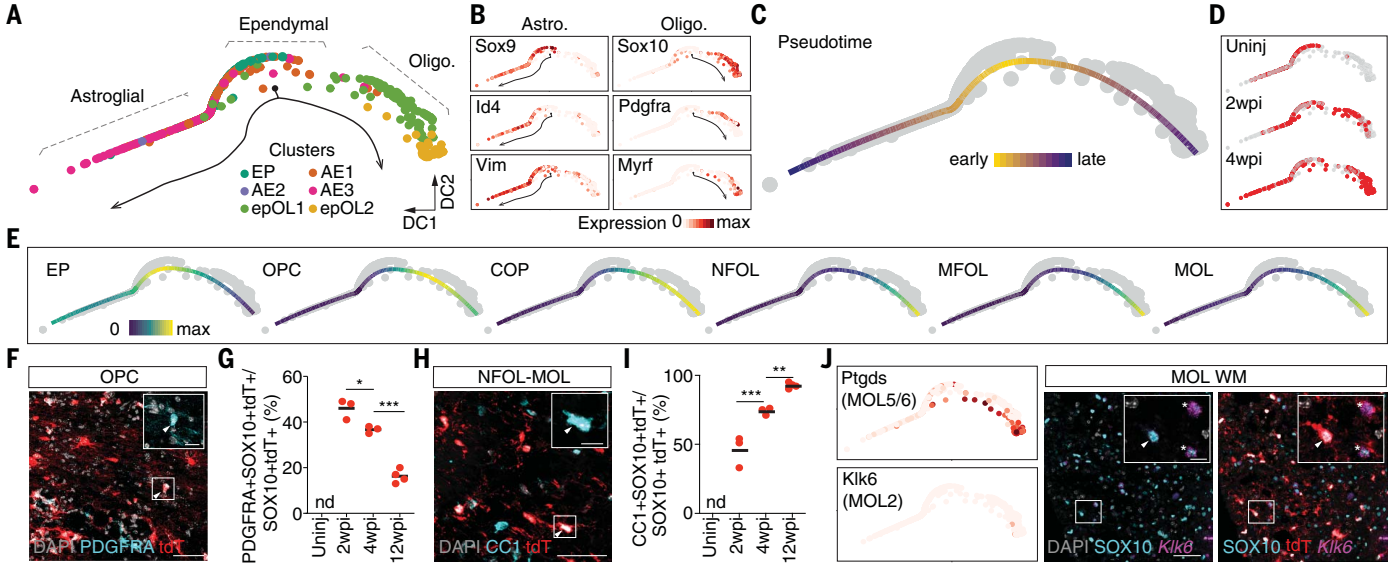

Fig. 4. Ependymal oligodendrogenesis recapitulates developmental oligodendrogenesis. (**A**) Diffusion map analysis of the injury response of fate-mapped ependymal cells from Foxj1-Olig2-tdT mice (uninjured, 2 wpi, and 4 wpi) captures the progression along two divergent branches. Cells are color-coded according to cluster identity (see Fig. 3H). (**B**) Expression of astrocyte and oligodendrocyte lineage genes defining each branch. (**C**) Diffusion map pseudotime projected onto the principal curve. (**D**) Sampling time matches pseudotime progression along both branches. (**E**) Signature scores for oligodendrocyte lineage stages projected onto the diffusion map principal curve show stepwise ependymal oligodendrogenesis. EP, ependymal; OPC, oligodendrocyte progenitor cell; COP, committed oligodendrocyte progenitor; NFOL, newly formed oligodendrocyte; MFOL, myelin-forming oligodendrocyte; MOL, mature oligodendrocyte. (**F** and **G**) Percentage of epOLs expressing the OPC marker PDGFRA over time (n = 3 or 4). (**H** and **I**) Percentage of epOLs expressing the mature OL marker CC1 over time (n = 3 or 4). (**J**) Mature epOLs express *Ptgds* and not *Klk6*, as shown in the projected expression in the diffusion map and RNAscope 12 weeks after injury. Asterisks show tdT-negative OLs expressing *Klk6* in the vicinity of tdT-positive epOLs. Arrowheads highlight some epOLs. WM, white matter. Scale bars, 50 μm (insets, 10 μm). Horizontal bar in (G) and (I) denotes the mean. *P < 0.05, **P < 0.01, ***P < 0.001 (one-way ANOVA followed by Tukey post hoc test).

This indicates that OLIG2 biases ependymal fate decisions early and that once commitment to an astroependymal or an oligodendrocyte fate takes place, cells progress further in the respective branch.

During developmental oligodendrogenesis, oligodendrocyte progenitors undergo a stepwise differentiation process that was recently characterized at the single-cell level (*19*). We calculated the scores for the top 50 gene expression signatures of the respective oligodendrocyte lineage maturation stage for every single cell from Foxj1-Olig2-tdT mice and projected it onto the principal curve trajectory (Fig. 4E) as well as whole-transcriptome correlation with each developmental maturation stage (fig. S11). This analysis revealed that as epOL cells progress in pseudotime along the oligodendrocyte lineage branch, they sequentially turn on and off the respective gene expression program in an orderly manner. This finding agrees with the observed progressive decrease of PDGFRA$^+$ and progressive increase in CC1$^+$ epOLs (Fig. 4, F to I). Lineage progression included, among other states, the transition through a proliferative OPC-like state that could be observed even 12 weeks after injury (Fig. 4E and fig. S10E); this suggests that the epOL population amplifies itself and could sustain itself without continuous ependymal cell input.

We observed that mature epOLs almost exclusively expressed the marker of mature oligodendrocyte subtype 5/6 (MOL5/6) *Ptgds* and not the mature oligodendrocyte subtype 2 (MOL2) marker *Klk6* (*20*), even in the vicinity of nonrecombined oligodendrocytes expressing *Klk6* (Fig. 4J); this finding implies that ependymal-derived oligodendrocytes acquired specific mature identities. We did not observe epOLs expressing the Schwann cell marker myelin protein zero (figs. S10F and S11). Thus, ependymal-derived oligodendrogenesis results in the production of transcriptionally mature oligodendrocytes.

Ependymal-derived oligodendrocytes remyelinate axons

To address whether mature epOLs were capable of remyelination, we studied their interaction with spared axons in spinal cord cross sections 3 months after a dorsal funiculus incision spinal cord injury (Fig. 5A). High-power confocal micrographs revealed that tdTomato membrane extensions colocalized with myelin basic protein (MBP) in axon wrappings, indicative of myelination (Fig. 5B). In sagittal sections, tdTomato sheaths from epOLs colocalized with the paranodal marker contactin-associated protein (CASPR), indicative of myelin formation (Fig. 5C). We next used expansion microscopy (*21*) to obtain further information regarding epOL axon ensheathment. To this end, we crossed Foxj1-Olig2-tdT mice with Thy1-GFP mice. Expansion of the tissue allowed reconstruction of epOL-axon contacts and revealed epOL ensheathment of axons (Fig. 5D and movie S1). Further, electron microscopy of the regions containing epOL-axon contacts revealed compact myelin formation from tdTomato-immunoreactive ependymal-derived oligodendrocytes (Fig. 5, E to G, and fig. S12). EpOLs thus participate in axon remyelination after injury.

Ependymal-derived oligodendrocytes support the recovery of axon conduction after injury

We thereafter turned to a clinically relevant moderate thoracic contusion model to further study the function of epOLs during injury repair. The response to the moderate contusion differed strikingly between Foxj1-Olig2-tdT and Foxj1-tdT mice (Fig. 6A), whereas the scarring and general locomotion remained similar (fig. S13, C to I). As a result of the larger affected area after contusion injury, the number of epOLs in Foxj1-Olig2-tdT mice increased by a factor of 3 in comparison to the dorsal funiculus incision model and exceeded by more than two orders of magnitude the number produced in Foxj1-tdT mice (32,000 ± 4900 SOX10$^+$ tdT$^+$ cells 12 weeks after injury; Fig. 6, B and C, and fig. S13, A and B). Relevant for potential

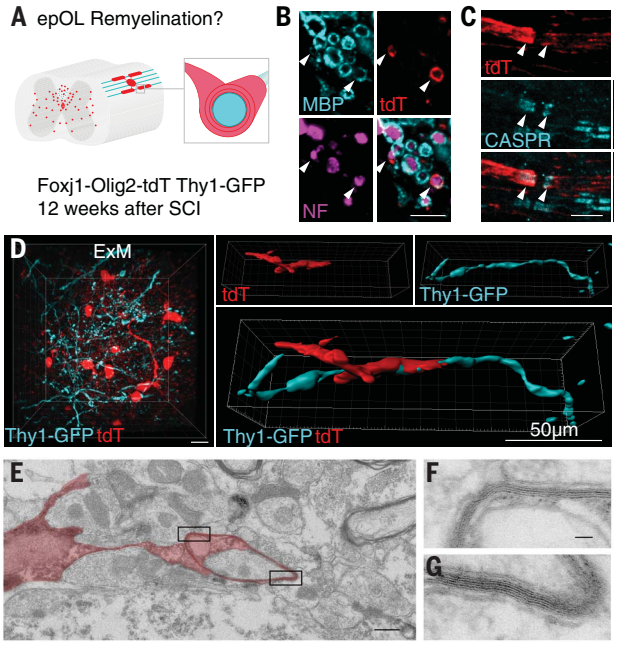

Fig. 5. Ependymal-derived oligodendrocytes contribute to remyelination. (**A**) Myelination analyses were performed in Foxj1-Olig2-tdT Thy1-GFP mice 12 weeks after dorsal funiculus incision injury. (**B**) Colocalization of tdTomato (tdT) and MBP wrapping axons stained against neurofilament (NF) (arrowheads). (**C**) epOL-derived myelin sheaths colocalize with the paranodal marker CASPR (arrowheads). (**D**) Expansion microscopy (ExM) shows axon wrapping by epOLs. Left: Example of a white matter area analyzed by ExM; epOLs in red, Thy1-GFP axons in cyan. Right: 3D reconstruction of a segmented inset showing wrapping of a Thy1-GFP neuronal process by a tdT-expressing epOL. (**E**) Electron micrograph of a tdT-immunoreactive cell and its process (red pseudocolor) initiating axon wrapping and myelination. Note the labeled cytoplasmic inner tongue of the epOL under the myelin sheath. (**F** and **G**) Compact myelin sheaths produced by the epOL at higher magnification from boxed areas in (E). Scale bars, 5 µm [(B) and (C)], 50 µm (D), 1 µm (E), 0.1 µm [(F) and (G)].

therapeutic strategies, tamoxifen administration starting 1 day after contusion led to oligodendrogenesis in a manner similar to pre-injury tamoxifen administration (fig. S14).

Axons that remain after a spinal cord injury can undergo substantial remyelination in rodents (*22*–*24*), but this process is protracted and incomplete; these axons often exhibit pathological myelin and aberrant conduction, and they can persist as electrically silent fibers chronically (*22*, *25*). Given that epOL generation had an additive effect over oligodendrocyte generation from OPCs (fig. S13, J to L), we studied whether epOLs could improve the recovery of axon conduction. Corticospinal neurons located in layer V of the motor cortex send descending fibers directly to the spinal cord. The descending fibers are part of the corticospinal tract (CST), synapse directly on motor neurons in the spinal cord, and are directly involved in motor control. To investigate whether epOL-derived remyelination could improve axon conduction in the CST after spinal cord injury, we performed electrophysiology in combination with optogenetics in vivo in anesthetized mice. To label and enable optogenetic activation of the CST, we injected an AAV expressing ChR2-EGFP (AAV9-CAG-ChR2-EGFP) or EGFP (AAV9-CAG-EGFP) as control into layer V of the motor cortex (*26*, *27*) (fig. S15, A to D).

Light-evoked compound action potential (optoCAP) volleys were detectable in the thoracic spinal cord at distances within at least 3 mm from the site of light delivery in mice expressing ChR2-EGFP in the CST (fig. S16, A and B) but were completely absent in mice expressing only EGFP (fig. S16C). In vivo measurement of the latency of the optoCAPs revealed a CST conduction velocity broadly concordant to the described slow conduction of the pyramidal tract in mice (4.57 ± 1.96 m/s; fig. S16, D to G) (*28*).

We next investigated optoCAPs and conduction velocities 12 to 14 weeks after contusion injury in Foxj1-Olig2-tdT mice and their Olig2-tdT littermates (controls not expressing Foxj1-creER), all expressing ChR2-EGFP in the CST. We applied optogenetic stimulation to the dorsal surface of the spinal cord two segments rostral to the lesion and recorded the induction of optoCAP immediately rostral or caudal to the epicenter of the lesion injury (Fig. 6D). We did not detect optoCAP induction in recordings caudal to the lesion in either group, owing to the sparsity of spared or regenerated CST axons (fig. S15B). Recordings immediately rostral to the lesion's epicenter revealed optoCAPs in most but not all mice (8/11 Foxj1-Olig2-tdT mice and 4/6 control mice; Fig. 6E). The same investigation was conducted in uninjured mice and revealed that optoCAPs could invariably be recorded at the same location in all animals (9/9 mice, tamoxifen-injected Foxj1-Olig2-tdT mice, and Olig2-tdT control mice; fig. S16G). The results indicate a partial CST conduction block in injured mice. Injured Olig2-tdT (control) mice displayed a severely reduced conduction velocity relative to uninjured counterparts (mean CST conduction velocity for injured controls was 19.0 ± 2.83% of the CST conduction velocity of uninjured mice; Fig. 6F). This reduction was partially rescued in injured Foxj1-Olig2-tdT mice (mean CST conduction velocity for injured Foxj1-Olig2-tdT mice was 27.9 ± 6.53% of the CST conduction velocity for uninjured mice; Fig. 6F). Last, we investigated the relationship between the conduction velocity and the level of CST remyelination in all injured mice. Conduction velocity was correlated to the percentage of myelin sheaths in the CST (Fig. 6, G and H). Together, our results support the idea that remyelination by newly recruited ependymal cell progeny can improve axon conduction after injury.

Discussion

Spontaneous cell replacement after injury is very limited. In both the brain and the spinal cord, the neural stem cells at large contribute only to astrogliogenesis after acute injuries (*2*). The apparent lineage restriction in stem cells has promoted the search for alternative sources for neuronal and oligodendroglial cell replacement, such as exogenous cell transplantation and direct reprogramming of local cell types (*3*). Here, in contrast, we show that there is a latent potential for cell replacement that enables their efficient recruitment for endogenous regeneration.

Injury was a requirement for the unfolding of the oligodendrocyte gene expression program, as we did not detect oligodendrogenesis from uninjured OLIG2-expressing ependymal cells. Injury-induced inflammatory mediators have been shown to facilitate lineage plasticity (*29*, *30*). Such signals might act by providing a required cofactor to facilitate OLIG2 access to chromatin, as reported for Brg1 (*31*), whose expression was injury-dependent in ependymal cells (fig. S6D). OLIG2 was predicted to have a DNA binding domain with possible pioneer activity based on its structure (*32*). We observed that OLIG2, when expressed in ependymal cells, may instead direct stimulus-dependent transcription factors to latent oligodendrocyte lineage enhancers, in a manner

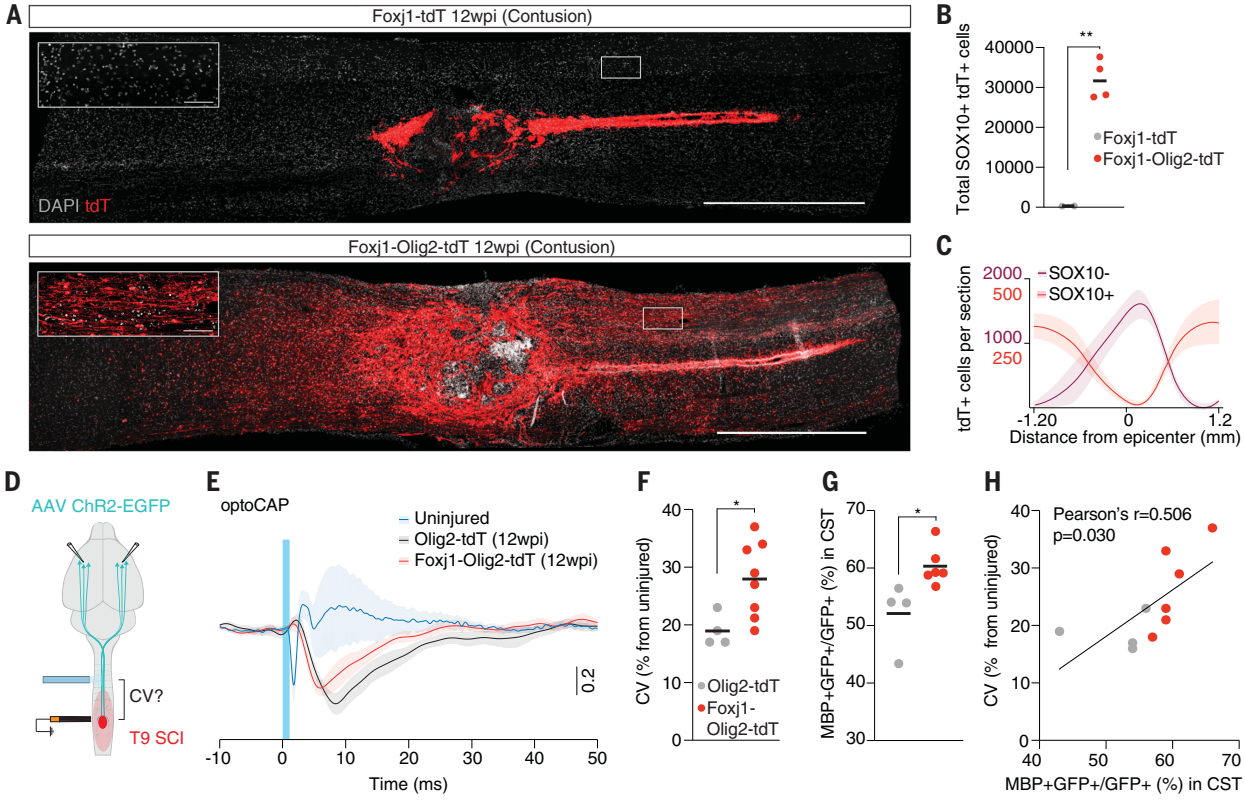

Fig. 6. Ependymal-derived oligodendrocytes support the recovery of axon conduction after injury. (**A**) Sagittal view of the injured spinal cord. Ependymal cells from Foxj1-tdT mice generate progeny that contribute to the astrocyte scar. The ependymal response is increased and spreads rostrocaudally in spared but reactive tissue in Foxj1-Olig2-tdT mice because of the generation of epOLs (inset). (**B**) Quantification of the total number of oligodendrocytes in the injured segment generated by ependymal cells 12 weeks after contusion SCI (n = 2 to 4). Horizontal bar denotes the mean. $^{**}P < 0.01$ [Student's t test, $t(4) = 8.570$]. (**C**) Linear regression analysis of the location of astroglial ($SOX10^-$) and oligodendroglial ($SOX10^+$) ependymal-derived cells with respect to the lesion epicenter in Foxj1-Olig2-tdT mice 12 weeks after contusion. Data are means ± SD (n = 4). (**D**) Schematic representation of the strategy to measure conduction velocity in the CST. AAV-CAG-ChR2-EGFP was injected in the motor cortex to label corticospinal neurons. Optical stimulation (473 nm) was applied two segments rostral to the lesion epicenter, and electrophysiological recordings were made above and below the lesion. (**E**) Average traces for the light-evoked compound action potential (optoCAP) in the CST in uninjured mice (Foxj1-Olig2-tdT and Olig2-tdT, blue, n = 9), injured controls (Olig2-tdT, gray, n = 4), and injured Foxj1-Olig2-tdT mice (red, n = 8). The blue vertical bar indicates the 2-ms light pulse. Shading indicates ±SEM. (**F**) Quantification of the conduction velocity (CV) in the CST in injured controls and injured Foxj1-Olig2-tdT mice measured immediately rostral to the lesion core. Horizontal bar denotes the mean. $^{*}P < 0.05$ [Student's t test, $t(10) = 2.551$]. (**G**) Quantification of the percentage of myelinated CST axons (MBP^+ GFP^+) from the total number of GFP^+ axons that survived in the 1.2 mm rostral to the epicenter in control (gray, n = 4) and Foxj1-Olig2-tdT (red, n = 6) mice. Horizontal bar denotes the mean. $^{*}P < 0.05$ [Student's t test, $t(7) = 2.984$]. (**H**) Regression analysis shows the correlation between conduction velocity and level of myelination in the CST. Scale bars, 1 mm (insets, 100 μm).

similar to that described for activity-induced enhancer selection in neurons (*33*). These latent enhancers might have been established during development when the progenitors of some ependymal cells express OLIG2 (*34*–*36*) and might have been maintained without sustained OLIG2 expression (*37*).

The need for enhanced remyelination extends to multiple neurological pathologies. Forebrain neural stem cells generate substantial numbers of oligodendrocytes after injury (*38*), and potential for a greater contribution exists (*39*). This greater potential suggests that latent accessibility of the oligodendrocyte program might be a feature of the adult stem cell pool; we have observed concordant chromatin profiles with ependymal cells at key loci (fig. S17). Parenchymal OPC–derived oligodendrogenesis and neural stem cell–derived oligodendrogenesis obey different signals (*39*), and neural stem cell–derived oligodendrocytes produced thicker myelin than that derived from parenchymal OPCs (*38*). We have further observed that ependymal-derived oligodendrogenesis can have an additive effect on OPC-derived oligodendrogenesis. This raises the possibility that neural stem cells and parenchymal progenitor oligodendrogenesis could be simultaneously enhanced, with potentially synergistic effects.

On average, 32,000 epOLs were generated after contusion spinal cord injury, which is comparable to the reported survival and integration of ~30,000 oligodendrocytes after transplantation (*40*). Regenerated axons are often unmyelinated (*41*), and promoting their conduction can enhance functional recovery (*42*). In addition, forced neuronal activity stimulates the recruitment of new oligodendrocytes for adaptive remyelination (*43*). The delivery of viral cargo in preclinical settings is undergoing rapid progress (*44*). It may be possible to deliver OLIG2 or manipulate its upstream regulators (*45*) to elicit ependymal oligodendrogenesis in a therapeutic setting. Combinatorial strategies aimed at promoting recovery of multiple cellular compartments simultaneously thus emerge as an attractive possibility.

Our work shows that the endogenous stem cell response can be engineered to generate cells with appropriate identity without compromising normal tissue recovery. Redirecting endogenous cell populations for cellular replacement to enhance the self-repair capacity

of the nervous system may thus be explored as a therapeutic alternative to cell transplantation.

REFERENCES AND NOTES

1. J. Silver, M. E. Schwab, P. G. Popovich, Central nervous system regenerative failure: Role of oligodendrocytes, astrocytes, and microglia. *Cold Spring Harb. Perspect. Biol.* **7**, a020602 (2014). doi: 10.1101/cshperspect.a020602; pmid: 25475091
2. J. Frisén, Neurogenesis and Gliogenesis in Nervous System Plasticity and Repair. *Annu. Rev. Cell Dev. Biol.* **32**, 127–141 (2016). doi: 10.1146/annurev-cellbio-111315-124953; pmid: 27298094
3. R. A. Barker, M. Götz, M. Parmar, New approaches for brain repair-from rescue to reprogramming. *Nature* **557**, 329–334 (2018). doi: 10.1038/s41586-018-0087-1; pmid: 29769670
4. E. J. Benner *et al*., Protective astrogenesis from the SVZ niche after injury is controlled by Notch modulator Thbs4. *Nature* **497**, 369–373 (2013). doi: 10.1038/nature12069; pmid: 23615612
5. M. Faiz *et al*., Adult Neural Stem Cells from the Subventricular Zone Give Rise to Reactive Astrocytes in the Cortex after Stroke. *Cell Stem Cell* **17**, 624–634 (2015). doi: 10.1016/j.stem.2015.08.002; pmid: 26456685
6. F. D. Miller, D. R. Kaplan, Mobilizing endogenous stem cells for repair and regeneration: Are we there yet? *Cell Stem Cell* **10**, 650–652 (2012). doi: 10.1016/j.stem.2012.05.004; pmid: 22704501
7. C. B. Johansson *et al*., Identification of a neural stem cell in the adult mammalian central nervous system. *Cell* **96**, 25–34 (1999). doi: 10.1016/S0092-8674(00)80956-3; pmid: 9989494
8. K. Meletis *et al*., Spinal cord injury reveals multilineage differentiation of ependymal cells. *PLOS Biol.* **6**, e182 (2008). doi: 10.1371/journal.pbio.0060182; pmid: 18651793
9. F. Barnabé-Heider *et al*., Origin of new glial cells in intact and injured adult spinal cord. *Cell Stem Cell* **7**, 470–482 (2010). doi: 10.1016/j.stem.2010.07.014; pmid: 20887953
10. A. T. Satpathy *et al*., Massively parallel single-cell chromatin landscapes of human immune cell development and intratumoral T cell exhaustion. *Nat. Biotechnol.* **37**, 925–936 (2019). doi: 10.1038/s41587-019-0206-z; pmid: 31375813
11. A. Zeisel *et al*., Molecular Architecture of the Mouse Nervous System. *Cell* **174**, 999–1014.e22 (2018). doi: 10.1016/j.cell.2018.06.021; pmid: 30096314
12. M.-I. Chung *et al*., Coordinated genomic control of ciliogenesis and cell movement by RFX2. *eLife* **3**, e01439 (2014). doi: 10.1093/nar/gkm727; pmid: 17897962
13. T. Werner, A. Hammer, M. Wahlbuhl, M. R. Bösl, M. Wegner, Multiple conserved regulatory elements with overlapping functions determine Sox10 expression in mouse embryogenesis. *Nucleic Acids Res.* **35**, 6526–6538 (2007). doi: 10.1093/nar/gkm727; pmid: 17897962
14. A. Antonellis *et al*., Identification of neural crest and glial enhancers at the mouse Sox10 locus through transgenesis in zebrafish. *PLOS Genet.* **4**, e1000174 (2008). doi: 10.1371/journal.pgen.1000174; pmid: 18773071
15. Q. R. Lu *et al*., Common developmental requirement for Olig function indicates a motor neuron/oligodendrocyte connection. *Cell* **109**, 75–86 (2002). doi: 10.1016/S0092-8674(02)00678-5; pmid: 11955448
16. Q. Zhou, D. J. Anderson, The bHLH transcription factors OLIG2 and OLIG1 couple neuronal and glial subtype specification. *Cell* **109**, 61–73 (2002). doi: 10.1016/S0092-8674(02)00677-3; pmid: 11955447
17. Y. Zhang *et al*., An RNA-sequencing transcriptome and splicing database of glia, neurons, and vascular cells of the cerebral cortex. *J. Neurosci.* **34**, 11929–11947 (2014). doi: 10.1523/JNEUROSCI.1860-14.2014; pmid: 25186741
18. P. Assinck, G. J. Duncan, B. J. Hilton, J. R. Plemel, W. Tetzlaff, Cell transplantation therapy for spinal cord injury. *Nat. Neurosci.* **20**, 637–647 (2017). doi: 10.1038/nn.4541; pmid: 28440805
19. S. Marques *et al*., Oligodendrocyte heterogeneity in the mouse juvenile and adult central nervous system. *Science* **352**, 1326–1329 (2016). doi: 10.1126/science.aaf6463; pmid: 27284195
20. E. M. Floriddia *et al*., Distinct oligodendrocyte populations have spatial preference and injury-specific responses. bioRxiv [preprint]. 6 July 2019.pmid: 580985
21. F. Chen, P. W. Tillberg, E. S. Boyden, Expansion microscopy. *Science* **347**, 543–548 (2015). doi: 10.1126/science.1260088; pmid: 25592419
22. Z. C. Hesp, E. Z. Goldstein, C. J. Miranda, B. K. Kaspar, D. M. McTigue, Chronic oligodendrogenesis and remyelination after spinal cord injury in mice and rats. *J. Neurosci.* **35**, 1274–1290 (2015). doi: 10.1523/JNEUROSCI.2568-14.2015; pmid: 25609641
23. P. Assinck *et al*., Myelinogenic Plasticity of Oligodendrocyte Precursor Cells following Spinal Cord Contusion Injury. *J. Neurosci.* **37**, 8635–8654 (2017). doi: 10.1523/JNEUROSCI.2409-16.2017; pmid: 28760862
24. B. E. Powers *et al*., Remyelination reporter reveals prolonged refinement of spontaneously regenerated myelin. *Proc. Natl. Acad. Sci. U.S.A.* **110**, 4075–4080 (2013). doi: 10.1073/pnas.1210293110; pmid: 23431182
25. N. D. James *et al*., Conduction failure following spinal cord injury: Functional and anatomical changes from acute to chronic stages. *J. Neurosci.* **31**, 18543–18555 (2011). doi: 10.1523/JNEUROSCI.4306-11.2011; pmid: 22171053
26. D. O. Dias *et al*., Reducing Pericyte-Derived Scarring Promotes Recovery after Spinal Cord Injury. *Cell* **173**, 153–165.e22 (2018). doi: 10.1016/j.cell.2018.02.004; pmid: 29502968
27. N. Jayaprakash *et al*., Optogenetic Interrogation of Functional Synapse Formation by Corticospinal Tract Axons in the Injured Spinal Cord. *J. Neurosci.* **36**, 5877–5890 (2016). doi: 10.1523/JNEUROSCI.4203-15.2016; pmid: 27225775
28. H. Tanaka, K. Ono, H. Shibasaki, T. Isa, K. Ikenaka, Conduction properties of identified neural pathways in the central nervous system of mice in vivo. *Neurosci. Res.* **49**, 113–122 (2004). doi: 10.1016/j.neures.2004.02.001; pmid: 15099709
29. J. Lee *et al*., Activation of innate immunity is required for efficient nuclear reprogramming. *Cell* **151**, 547–558 (2012). doi: 10.1016/j.cell.2012.09.034; pmid: 23101625
30. L. Mosteiro *et al*., Tissue damage and senescence provide critical signals for cellular reprogramming in vivo. *Science* **354**, aaf4445 (2016). doi: 10.1126/science.aaf4445; pmid: 27884981
31. Y. Yu *et al*., Olig2 targets chromatin remodelers to enhancers to initiate oligodendrocyte differentiation. *Cell* **152**, 248–261 (2013). doi: 10.1016/j.cell.2012.12.006; pmid: 23332759
32. A. Soufi *et al*., Pioneer transcription factors target partial DNA motifs on nucleosomes to initiate reprogramming. *Cell* **161**, 555–568 (2015). doi: 10.1016/j.cell.2015.03.017; pmid: 25892221
33. T. Vierbuchen *et al*., AP-1 Transcription Factors and the BAF Complex Mediate Signal-Dependent Enhancer Selection. *Mol. Cell* **68**, 1067–1082.e12 (2017). doi: 10.1016/j.molcel.2017.11.026; pmid: 29272704
34. N. Masahira *et al*., Olig2-positive progenitors in the embryonic spinal cord give rise not only to motoneurons and oligodendrocytes, but also to a subset of astrocytes and ependymal cells. *Dev. Biol.* **293**, 358–369 (2006). doi: 10.1016/j.ydbio.2006.02.029; pmid: 16581057
35. H. Fu *et al*., Molecular mapping of the origin of postnatal spinal cord ependymal cells: Evidence that adult ependymal cells are derived from Nkx6.1^{+} ventral neural progenitor cells. *J. Comp. Neurol.* **456**, 237–244 (2003). doi: 10.1002/cne.10481; pmid: 12528188
36. W. D. Richardson, N. Kessaris, N. Pringle, Oligodendrocyte wars. *Nat. Rev. Neurosci.* **7**, 11–18 (2006). doi: 10.1038/nrn1826; pmid: 16371946
37. G. C. Hon *et al*., Epigenetic memory at embryonic enhancers identified in DNA methylation maps from adult mouse tissues. *Nat. Genet.* **45**, 1198–1206 (2013). doi: 10.1038/ng.2746; pmid: 23995138
38. Y. L. Xing *et al*., Adult Neural Precursor Cells From the Subventricular Zone Contribute Significantly to Oligodendrocyte Regeneration and Remyelination. *J. Neurosci.* **34**, 14128–14146 (2014), doi: 10.1038/nature14957; pmid: 26416758
39. J. Samanta *et al*., Inhibition of Gli1 mobilizes endogenous neural stem cells for remyelination. *Nature* **526**, 448–452 (2015). doi: 10.1038/nature14957; pmid: 26416758
40. A. Yasuda *et al*., Significance of remyelination by neural stem/progenitor cells transplanted into the injured spinal cord. *Stem Cells* **29**, 1983–1994 (2011). doi: 10.1002/stem.767; pmid: 22028197
41. L. T. Alto *et al*., Chemotropic guidance facilitates axonal regeneration and synapse formation after spinal cord injury. *Nat. Neurosci.* **12**, 1106–1113 (2009). doi: 10.1038/nn.2365; pmid: 19648914
42. F. Bei *et al*., Restoration of Visual Function by Enhancing Conduction in Regenerated Axons. *Cell* **164**, 219–232 (2016). doi: 10.1016/j.cell.2015.11.036; pmid: 26771493
43. E. M. Gibson *et al*., Neuronal activity promotes oligodendrogenesis and adaptive myelination in the mammalian brain. *Science* **344**, 1252304 (2014). doi: 10.1126/science.1252304; pmid: 24727982
44. E. Hudry, L. H. Vandenberghe, Therapeutic AAV Gene Transfer to the Nervous System: A Clinical Reality. *Neuron* **101**, 839–862 (2019). doi: 10.1016/j.neuron.2019.02.017; pmid: 30844402
45. E. Dessaud *et al*., Interpretation of the sonic hedgehog morphogen gradient by a temporal adaptation mechanism. *Nature* **450**, 717–720 (2007). doi: 10.1038/nature06347; pmid: 18046410

ACKNOWLEDGMENTS

We thank the Karolinska Center for Transgene Technologies (KCTT) for mouse generation, S. Edwards from the Advanced Light Microscopy Facility at SciLifeLab for help with light sheet microscopy, S. Giatrellis for help with flow cytometry, the Swedish National Infrastructure for Computing through Uppsala Multidisciplinary Center for Advanced Computational Science (UPPMAX) for computational resources, and L. Buades for preparing graphical illustrations. **Funding:** Supported by Human Frontiers Science Programme long-term fellowship LT001040/2017 (E.L.-B.), a Marie Sklodowska-Curie Action fellowship (J.M.C.), and grants from the Swedish Research Council, the Swedish Cancer Society, the Swedish Foundation for Strategic Research, Knut och Alice Wallenbergs Stiftelse, the Strategic Research Programme in Stem Cells and Regenerative Medicine at Karolinska Institutet (StratRegen), Hjärnfonden, St. Petersburg University grant ID 51132811, Karolinska Institutet, the Torsten Söderbergs Stiftelse, and the Wings for Life Spinal Cord Research Foundation. **Author contributions:** Conceptualization, J.F., J.M.C., and E.L.-B.; methodology, E.L.-B., J.M.C., P.L.M., O.S., M.C., and J.F.; software, M.Z., E.L.-B., J.B., and P.L.M.; formal analysis, E.L.-B., M.Z., J.B., and P.L.M.; investigation, E.L.-B., Y.W., J.M.C., P.L.M., E.S., O.S., and M.S.; electron microscopy, O.S. and E.S.; data curation, M.Z., J.B., Y.W., and E.L.-B.; writing–original draft, E.L.-B.; writing–review and editing, J.F. and all authors; visualization, E.L.-B., P.L.M., M.Z., and J.B.; funding acquisition, J.F., M.C., O.S., and J.L.; supervision, J.F. **Competing interests:** E.L.-B., J.B., J.L., and J.F. are consultants to 10X Genomics. J.M.C. is currently employed by 10X Genomics. **Data and materials availability:** All raw sequencing data in the study as well as filtered gene expression and chromatin accessibility matrices have been deposited in Gene Expression Omnibus (GEO) under accession number GSE148316.

SUPPLEMENTARY MATERIALS

science.sciencemag.org/content/370/6512/eabb8795/suppl/DC1
Materials and Methods
Figs. S1 to S17
Table S1
References (*46*–*75*)
Data S1 to S3
Movie S1
MDAR Reproducibility Checklist

View/request a protocol for this paper from *Bio-protocol*.

24 March 2020; accepted 4 August 2020
10.1126/science.abb8795

A latent lineage potential in resident neural stem cells enables spinal cord repair

Enric Llorens-Bobadilla, James M. Chell, Pierre Le Merre, Yicheng Wu, Margherita Zamboni, Joseph Bergenstråhle, Moa Stenudd, Elena Sopova, Joakim Lundeberg, Oleg Shupliakov, Marie Carlén and Jonas Frisén

Science **370** (6512), eabb8795.
DOI: 10.1126/science.abb8795

Spinal cord stem cells

Injuries to the mammalian spinal cord do not heal easily. Llorens- Bobadilla *et al.* studied mouse ependymal cells, which function as stem cells for the spinal cord (see the Perspective by Becker and Becker). Chromatin accessibility and transcriptomic assays revealed that these cells carry a latent ability to differentiate into oligodendrocytes, which is much needed for remyelination of axons around an injury. The ependymal cells were triggered to differentiate into oligodendrocytes by expression of the oligodendrocyte lineage transcription factor OLIG2. Expression of OLIG2 in ependymal cells specifically and inducibly enabled the production of oligodendrocytes. The ependymal-derived oligodendrocytes aided axon remyelination and improved axon conduction after spinal cord injury.

Science, this issue p. eabb8795; see also p. 36